Investigating trends in proton single-particle states in $Z = 51$ isotopes using transfer reactions

2012 J. Phys.: Conf. Ser. 381 012099

(http://iopscience.iop.org/1742-6596/381/1/012099)

Investigating trends in proton single-particle states in $Z = 51$ isotopes using transfer reactions

A J Mitchell[1], S J Freeman[1], J P Schiffer[2], J A Clark[2], C M Deibel[2,3], C R Hoffman[2], A M Howard[1], B P Kay[2], P D Parker[4], D K Sharp[1] and J S Thomas[1]

[1] Schuster Laboratory, University of Manchester, Manchester, M13 9PL, UK
[2] Physics Division, Argonne National Laboratory, Argonne, IL 60439, USA
[3] Joint Institute for Nuclear Astrophysics, Michigan State University, East Lansing, MI 48824, USA
[4] A. W. Wright Nuclear Structure Laboratory, Yale University, New Haven, CT 06520, USA

E-mail: alan.mitchell@postgrad.manchester.ac.uk

Abstract. A study of low-lying excited states in $Z = 51$ isotopes has been performed using single-proton adding reactions, (α,t) and (^{3}He,d), on the series of stable, even mass $Z = 50$ isotopes. Our goal was to build upon results from a previous (α,t) study [1] by examining the fragmentation of high-j ($g_{7/2}$ and $h_{11/2}$) single-proton strengths utilising greater statistics. Data from the (^{3}He,d) measurements provide further information regarding the low-j orbitals within this nuclear shell. Preliminary findings from the analysis are presented in this report.

Introduction

A recent study investigated the behaviour of the single-proton states in $Z = 51$ isotopes [1]. Low-lying, excited states were populated in these nuclei using (α,t) reactions. Spectroscopic factors of the lowest-lying states corresponding to $\ell = 4$ ($g_{7/2}$) and $\ell = 5$ ($h_{11/2}$) transfer were found to be consistent to within $\pm15\%$ across the isotopes and appeared to be near-single-particle-like in nature. Hence, the energy of these states could be used as a good approximation to the energy centroid of the underlying single-particle orbitals. It was found that the separation in energy of these lowest-lying $\ell = 4$ and $\ell = 5$ states increased by approximately 1 MeV from $^{113-125}$Sb. As these two node-less, single-particle orbitals possess similar radial overlap integrals, any smooth variation in potential or increased filling of neutron levels would effect each orbital in a similar fashion.

A later paper [2], describing the evolution of nuclear shells due to the tensor interaction, included calculations involving the $\pi g_{7/2}$ and $\pi h_{11/2}$ orbitals in $Z = 51$ isotopes. The trends in these calculations were found to be very well matched to the experimental data of Ref. [1] (see Figure 1), indicating that it is the effects of the tensor interaction that are driving the evolution of these single-proton orbitals, as neutrons fill predominantly the $\nu h_{11/2}$ in the Sn cores. A lack of statistics prohibited a detailed analysis of the small fragments of single-particle strength from being performed using the data in Ref. [1]. The aim of this study is to investigate the

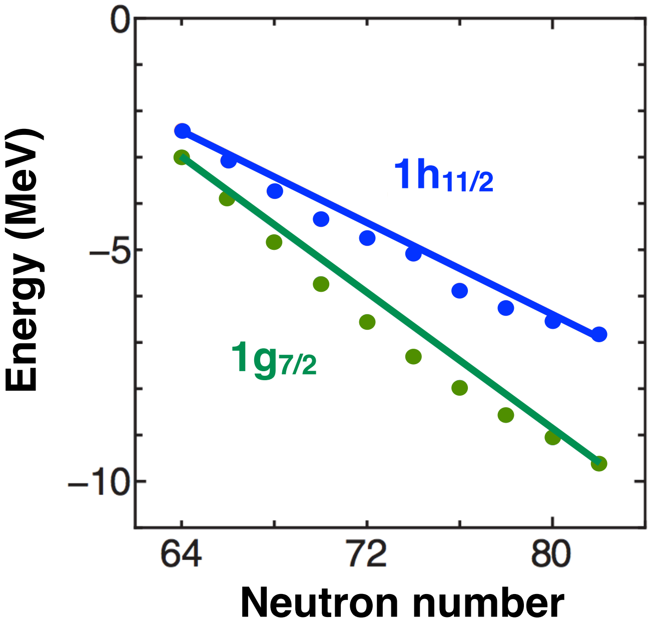

Figure 1. (Colour online) Trends in proton effective single-particle energies in $Z = 51$ isotopes. Points are from experimental data of Ref. [1]. Solid lines are theoretical calculations published in Ref. [2]. Figure has been adapted from Ref. [2].

fragmentation of the $\pi g_{7/2}$ and $\pi h_{11/2}$ single-particle strength in more detail through the use of greater statistics from (α,t) reactions, while gaining additional information on the low-j states located within the nuclear shell ($s_{1/2}$ and $d_{3/2,\ 5/2}$) via (^{3}He,d) reactions.

The behaviour of the tensor force is dependent upon the orientations of the spins of interacting nucleons. Its effect depends on the sense of the spin-orbit coupling, with different consequences for $j_>$ ($\ell + s$) and $j_<$ ($\ell - s$) states. The effect between $j_<$ $j_<$ (or $j_>$ $j_>$) pairs is repulsive, whereas the effect between $j_<$ $j_>$ (or vice-versa) is attractive. These are enhanced for orbitals possessing similar radial overlap integrals and those with high ℓ. Spectroscopic data from ^{A}Sn(d,p)$^{A+1}$Sn measurements [4] indicate that neutrons predominantly fill the $\nu h_{11/2}$ orbital with increasing neutron number (see Figure 2). The result of this, when considering the behaviour of the $\pi g_{7/2}$ and $\pi h_{11/2}$ orbitals, is that the $g_{7/2}$ orbital is lowered in energy whereas the energy of the $h_{11/2}$ is raised. This is observed experimentally as an increase in the separation of the energies of the orbitals.

Experiment

This series of experiments was performed at the A. W. Wright Nuclear Structure Laboratory (WNSL), Yale University. Helium beams were accelerated by the ESTU tandem Van de Graaff accelerator [5]. Light reaction products were momentum analysed using the Enge split pole spectrometer [6] before detection using a gas-filled ionisation chamber followed by a plastic scintillator. Two energy-loss signals from the focal plane detectors give particle identification, and particle momentum was determined using position signals from front wires on the ionisation chamber utilising a delay line method. A sub-Coulomb barrier 15-MeV α-particle beam was used with the spectrometer set at 20° to measure elastic scattering. This set up is consistent with Rutherford scattering to within 1% and allowed accurate determination of the product of target thickness and spectrometer aperture size. The aperture size remained fixed throughout the experiments to minimise systematic errors. For the single-proton adding reactions, a 37.5-MeV α-particle beam was used for the (α,t) reactions, and a 25-MeV ^{3}He beam for the (^{3}He,d)

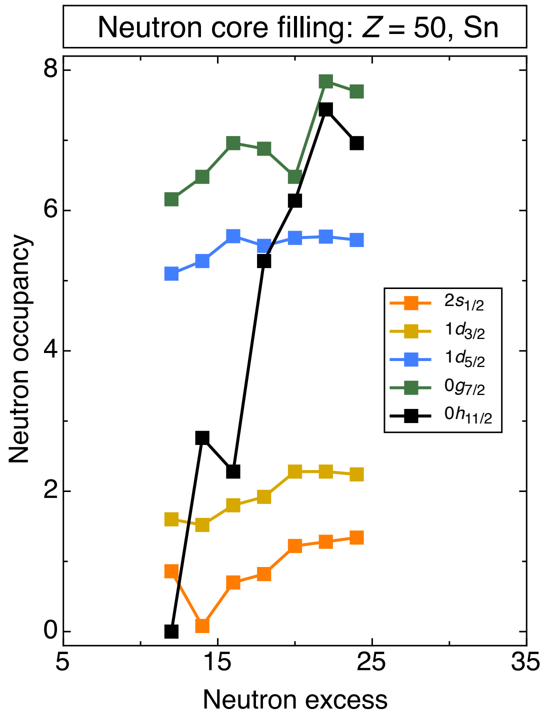

Figure 2. (Colour online) Occupancies of neutrons in $Z = 50$ cores with increasing neutron number; derived from spectroscopic information in Ref. [4]. Occupation of $h_{11/2}$ orbital increases rapidly in comparison to the other orbitals.

measurements. The energies were chosen to be sufficiently above the Coulomb barrier in the entrance and exit channels. Typical beam currents used were ∼70-100 enA. The (α,t) measurements were taken at 6° and 18°, with the $(^3\mathrm{He},d)$ measurements taken at 6° and 15°. The angles was chosen as they corresponds to maxima in the angular distributions where assumptions made in the DWBA calculations are best met and it is possible to discriminate between different degrees of ℓ-transfer in each reaction.

Isotopically enriched $^{112-124}$Sn targets used were typically ∼200 μg/cm^2 thick, evaporated onto a ∼50 μg/cm^2 carbon backing. Contaminant peaks in the spectra due to reactions on ^{12,13}C and ^{16}O in the targets were not present in the (α,t) measurement due to the large difference in rigidities of the tritons from these reactions compared to those from the reactions of interest. This was not the case in the $(^3\mathrm{He},d)$ where contaminant peaks from reactions on C and O obscured a number of states of interest.

Current analysis

Examples of focal plane spectra obtained from each reaction are shown in Figure 3. These were calibrated for energy using previously known states [7]. States identified as corresponding to high-ℓ transfer are dominant in the (α,t) spectra. Conversely, states corresponding to low-ℓ transfer are dominant in the $(^3\mathrm{He},d)$ spectra. This is due to the varying momentum matching conditions of each reaction. Typical energy resolution of the spectra was between 40-70 keV. Cross sections were determined from the yield of each identified state in the focal plane spectra by normalising them to the target thickness and beam current.

Quantum numbers for the transferred angular momentum are assigned on the basis of measured angular distributions compared to the results of distorted wave Born approximation (DWBA)

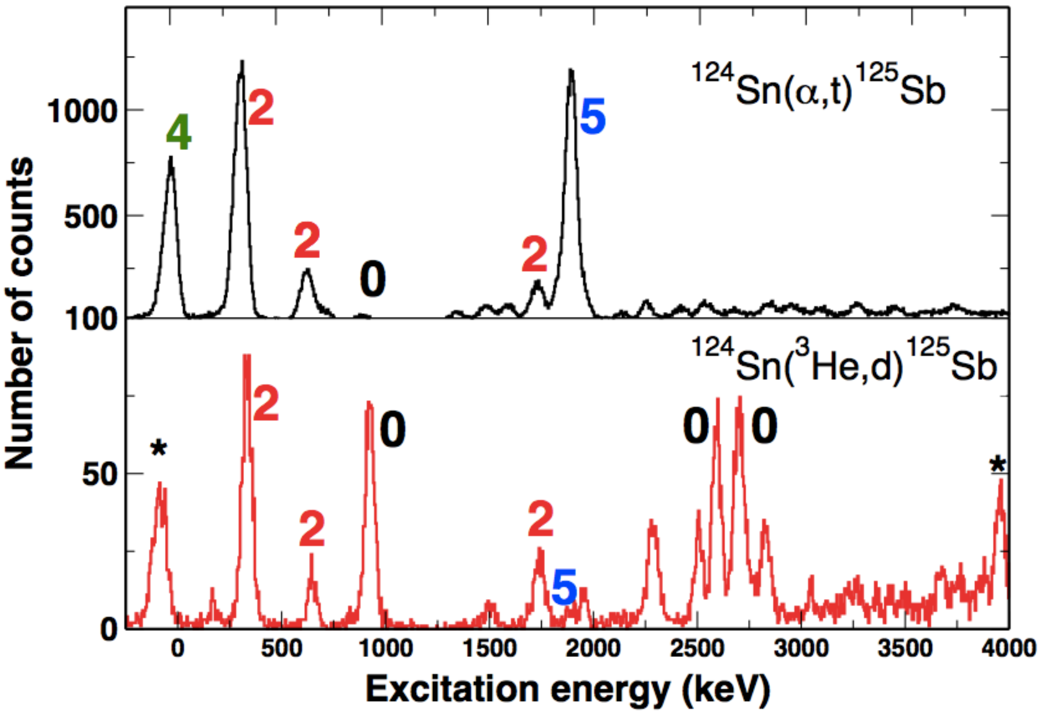

Figure 3. (Colour online) Energy calibrated particle spectra of (α,t) and (^{3}He,d) reactions on ^{124}Sn target at 6°. Examples of peaks corresponding to different ℓ-transfer values are labeled; * indicates contamination from carbon and oxygen in the targets.

calculations. The DWBA cross sections were calculated with the finite-range code PTOLEMY [8]. The analysis presented in this report has been carried out using the following sets of optical model parameters: fixed potentials of Ref. [9] were used for He species; those of Ref. [10] for tritons and global potentials of Ref. [11] for deuterons. A full survey of the effect of using different optical-model parameter sets is ongoing. The calculated angular distributions were normalised to the experimental cross sections and used to determine the ℓ-transfer for that particular state. For a number of states, particularly those more weakly populated, these two-point distributions possess a degree of ambiguity. By plotting ratios of cross sections, such as $\sigma_{(\alpha,t)}(18°)$ / $\sigma_{(^3\mathrm{He},d)}(15°)$ vs $\sigma_{(^3\mathrm{He},d)}(6°)$ / $\sigma_{(^3\mathrm{He},d)}(15°)$, we obtain an additional tool which aids this process. Examples of angular distributions and ratios are shown in Figure 4. This combination of angular distributions and ratio plots has proven successful in making ℓ-transfer assignments. For the (α,t) measurements, assignments of previously known $\ell = 4$ and $\ell = 5$, in general, agree with the assignments made in this study on the assumption that these transitions lead to the population of $7/2^+$ and $11/2^-$ states respectively. In the (^{3}He,d) data, the same is true for the $\ell = 0$ assignments ($1/2^+$). Both reactions are reasonably well matched for $\ell = 2$ transitions, populating both $3/2^+$ and $5/2^+$ states. Without the advantage of polarised beam data, it is not possible to distinguish between $3/2^+$ and $5/2^+$ states as the shapes of the angular distributions are the same. For the current analysis, all $\ell = 2$ states have been considered together.

Spectroscopic factors have been determined for each state using a DWBA analysis, where they are normalised such that the total strength for a particular orbital sums to 100% according to the sum rules for transfer reactions [12]. A normalisation across all targets for the $\ell = 2$, 4

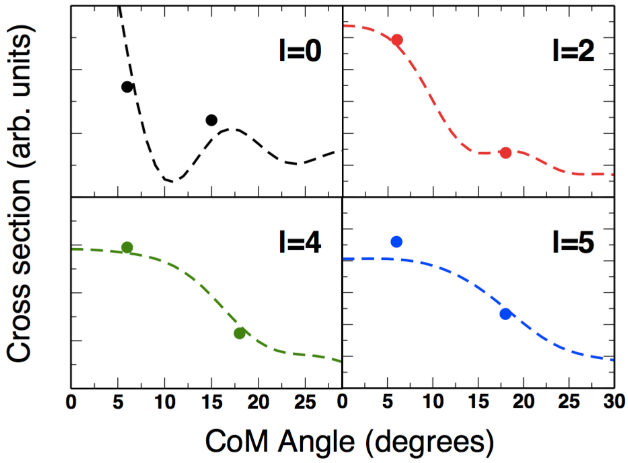

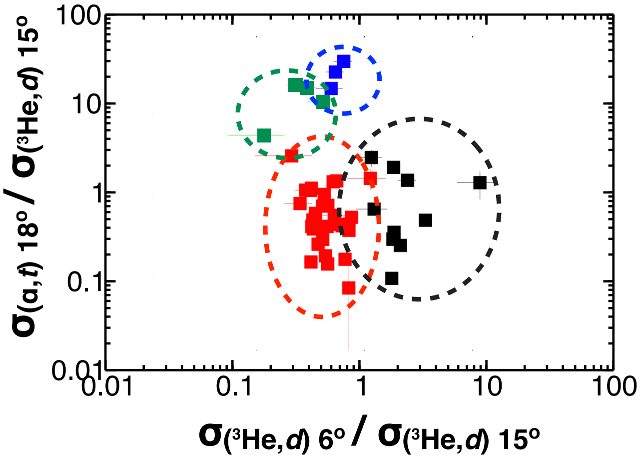

Figure 4. (Colour online) (Top) Examples of angular distributions for reactions on ^{124}Sn target allowing ℓ-transfer assignments. $\ell = 0$ data from (^{3}He,d) measurements; $\ell = 2$, 4 and 5 data from (α,t) measurements. Dashed lines are calculated angular distributions of best-suited ℓ-transfer. Points are experimental cross sections. Statistical errors are smaller than the size of the points. (Botom) $\sigma_{(\alpha,t)}(18^\circ)$ / $\sigma_{(^3\mathrm{He},d)}(15^\circ)$ vs $\sigma_{(^3\mathrm{He},d)}(6^\circ)$ / $\sigma_{(^3\mathrm{He},d)}(15^\circ)$. States corresponding to a particular ℓ-transfer tend to cluster together and using known states this aids in the identification of unknown states. Data taken from states where cross sections were measured in both reactions at both angles.

and 5 states from (α,t) measurements was determined. A separate normalisation was used for the $\ell = 0$ states from (^{3}He,d) data. In general, the summed strengths have been found to be consistent to within $\sim$15%, which is within the estimated errors of these quantities.

Figure 5 shows the summed strengths of the $7/2^+$ and $11/2^-$ states, and they have been found to be consistent across the chain of isotopes. Also plotted is the spectroscopic factor of the dominant, lowest-lying state in each isotope for comparison as this was considered in Ref. [1]. The dominant $\ell = 4$ and $\ell = 5$ states in each isotope have been found to hold between 60-80% of the total single-particle strength when all the observed fragments are considered.

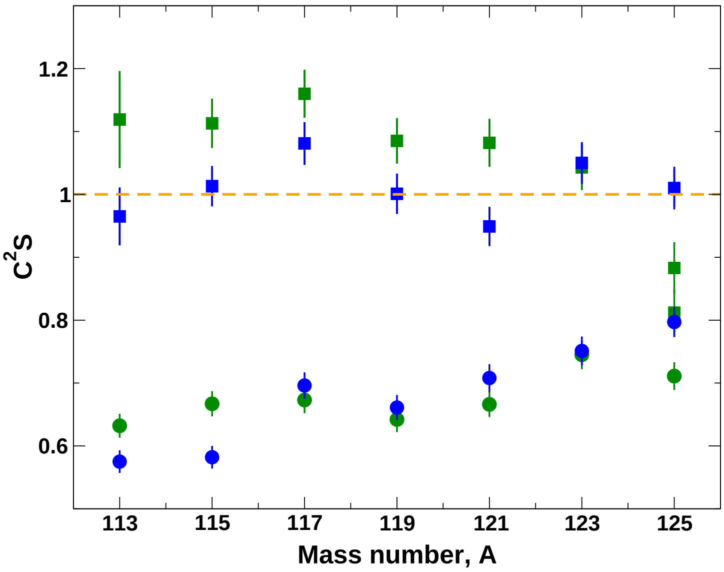

Figure 5. (Colour online) Spectroscopic factors of $\ell = 4$ (green) and $\ell = 5$ (blue) transfer for all isotopes. Square points are summed spectroscopic strengths, circle points are the spectroscopic factor of the lowest-lying state in each isotope. Error bars represent statistical uncertainties.

Conclusion

In conclusion, proton single-particle states have been populated in $Z = 51$ isotopes via (α,t) and $(^3\mathrm{He},d)$ reactions. Low-lying, excited states populated in these isotopes have been identified and their associated ℓ-transfer determined via a DWBA analysis. Spectroscopic factors have been determined for these states and the summed spectroscopic strengths have been found to be constant across the chain. Preliminary findings indicate that the identified fragmentation of single-particle strength does not substantially alter the previous conclusions [1]. A more detailed analysis is forthcoming.

This work was funded by the US Department of Energy, Office of Nuclear Physics, under Contract Nos. DE-AC02-06CH11357 and DE-FG02-04ER41320, NSF Grant No. PHY-08022648, and the UK Science and Technology Facilities Council.

References

[1] Schiffer J P *et al.* 2004 *Phys. Rev. Lett.* **92**, 162501
[2] Otsuka T *et al.* 2005 *Phys. Rev. Lett.* **95**, 232502
[3] Yukawa Y H 1935 *Proc. Phys. Math. Soc. Japan* **17**, 48
[4] Schneid E J, Prakash A, and Cohen B L 1967 *Phys. Rev.* **156**, 1316; Bechara M J and Dietzsch O 1975 *Phys. Rev.* C **12**, 90; Nealy C L and Sheline R K 1964 *Phys. Rev.* **135**, B325
[5] Hyder H R M *et al.* 1988 *Nucl. Instrum. Methods* A **268**, 285
[6] Spencer J E and Enge H A 1967 *Nucl. Instrum. Methods* **49**, 181
[7] Conjeaud M *et al.* 1968 *Nuclear Physics* A **117**, 449-471
[8] Macfarlane M H and Pieper S C 1978 *Argonne National Laboratory Report* ANL-76-11
[9] Bassani G and Picard J 1969 *Nuclear Physics* A **131**, 653
[10] Flynn E R, Brown R E, Ajzenberg-Selove F, and Cizewski J A 1983 *Phys. Rev.* C **28**, 575
[11] Perey C M and Perey F G 1966 *Phys. Rev.* **152**, 923
[12] Macfarlane M H and French J B 1960 *Rev. Mod. Phys.* **32**, 567